Eur Radiol (2005) 15: 1934–1947
DOI 10.1007/s00330-005-2734-9

PHYSICS

Martin Spahn

Flat detectors and their clinical applications

Received: 22 November 2004
Revised: 8 February 2005
Accepted: 1 March 2005
Published online: 2 April 2005

M. Spahn (✉)
Siemens AG, Medical Solutions,
Angiography, Fluoroscopic and
Radiography Systems,
Siemensstraße 1,
91301 Forchheim, Germany
e-mail: martin.spahn@siemens.com
Tel.: +49-9191-188704
Fax: +49-9191-189877

Abstract Diagnostic and interventional flat detector X-ray systems are penetrating the market in all application segments. First introduced in radiography and mammography, they have conquered cardiac and general angiography and are getting increasing attention in fluoroscopy. Two flat detector technologies prevail. The dominating method is based on an indirect X-ray conversion process, using cesium iodide scintillators. It offers considerable advantages in radiography, angiography and fluoroscopy. The other method employs a direct converter such as selenium which is particularly suitable for mammography. Both flat detector technologies are based on amorphous silicon active pixel matrices. Flat detectors facilitate the clinical workflow in radiographic rooms, foster improved image quality and provide the potential to reduce dose. This added value is based on their large dynamic range, their high sensitivity to X-rays and the instant availability of the image. Advanced image processing is instrumental in these improvements and expand the range of conventional diagnostic methods. In angiography and fluoroscopy the transition from image intensifiers to flat detectors is facilitated by ample advantages they offer, such as distortion-free images, excellent coarse contrast, large dynamic range and high X-ray sensitivity. These characteristics and their compatibility with strong magnetic fields are the basis for improved diagnostic methods and innovative interventional applications.

Keywords Flat detector · Amorphous silicon active matrix · Radiography · Angiography · Digital image processing

Introduction

In the late 1990s—about 100 years after the discovery of X-rays by Wilhelm Conrad Röntgen—flat detectors were first introduced in medical X-ray diagnostics. Since then this new technology has set out to become the prime standard in digital X-ray imaging. In general projection radiography and mammography flat detectors are increasingly replacing the analog screen-film combinations as well as the digital storage phosphor systems. In cardiac angiography flat detectors with the characteristics of real-time imaging of up to 30 fps (frames per second) or even 60 fps in pediatric cardiac imaging have become so popular that they have almost completely substituted the image intensifier systems within a few years. Changes of this nature are also taking place in general angiography and in fluoroscopy. Hence, flat detectors put us for the first time in a position to finally realize the vision of obtaining a single technology that covers all applications in X-ray diagnostics and interventional techniques [1–7].

In the following, the technology of flat detectors is introduced and their two flavors of indirect and direct conversion are discussed. Next, the basic performance characteristics of flat detectors is presented. Thereafter, the main advan-

tages provided by this technology are discussed with the focus on workflow, image processing and new applications. Finally, a brief outlook into future developments is given.

Technology and design of flat detectors

Any X-ray detector for medical imaging needs to serve the purpose of efficiently absorbing the impinging X-ray flux and converting it into a geometry-conserving digital image signal. The spatial and contrast resolution of the detector should be selected to meet the requirements of the respective application. While the signal per absorbed X-ray should be maximized, the additive electronic noise generated during the numerous conversion and amplification steps is to be kept at a minimum. DQE (detective quantum efficiency) has evolved as the fundamental physical parameter describing the performance characteristics of an X-ray detector as it combines these various requirements. It describes a detector's ability to convert efficiently the available X-ray radiation at its input into a useful image signal at its output [8]. The objective of any advances in the development of detector technology must be either to reach or to surpass the DQE of previously established detector technologies.

A number of design criteria directly influence the main features of a detector. They include (1) active area, (2) pixel size, (3) image acquisition rate, (4) dynamic range, as well as (5) outer dimensions and (6) weight. All of these parameters need to be selected carefully in accordance with the intended application of the detector.

Flat detector technology is the only detector technology available today that covers the various requirements of the entire application spectrum, ranging from general radiography to mammography, angiography and fluoroscopy. In the following sections, flat detector technology is described and discussed in detail.

The amorphous silicon active readout matrix

The development of LCD (liquid crystal display) technology for the consumer market as a replacement for monitors based on cathode ray tubes, has made a technology available whose characteristics are also ideally suited for sensors in medical X-ray imaging. It is based on hydrogenated amorphous silicon (a-Si:H) which can be deposited as thin films. Amorphous silicon combines several favorable characteristics. First, it exhibits all of the semiconductor properties such as doping, photoconductivity or junction formation. This makes it suitable for the manufacture of electrical components such as TFTs (thin-film transistors) and photodiodes. Second, the plasma deposition process permits large-area deposition which allows to produce active matrices of several million pixels (Fig. 1) and sizes exceeding 40×40 cm^2. Third, amorphous silicon has proven to be highly radiation hard, making it suitable for applications in medical X-ray imaging. These active matrices are the central components of flat detectors.

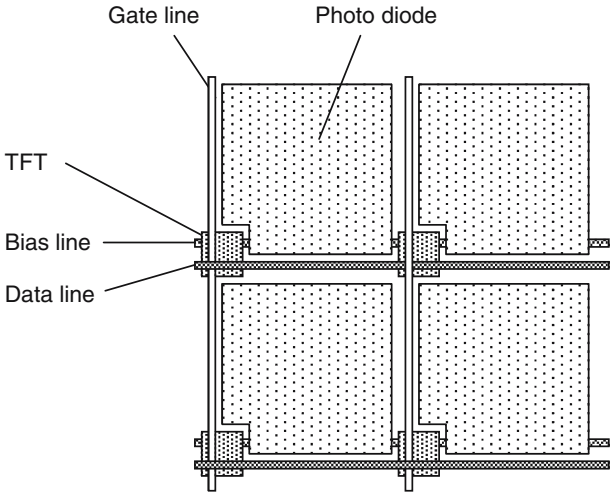

Fig. 1 Schematic view of the pixel structure of an indirect converting amorphous silicon active matrix sensor array showing photodiode, TFT, as well as gate, bias and data lines

Two different conversion processes of X-ray radiation into electric charge prevail. The first approach is based on an indirect conversion process, where the X-ray radiation is converted into light which in turn is absorbed, creating electric charge. The second approach features the direct conversion of X-ray quanta into electric charge. Both methods are described in the following sections.

Flat detectors based on an indirect conversion process

The most widely used design of flat detectors as of today is based on a two-level, indirect conversion process [9–13]. The X-ray quantum is absorbed creating a high energy electron via photo absorption (Fig. 2). While losing energy in the scintillator material, the electron creates a large number

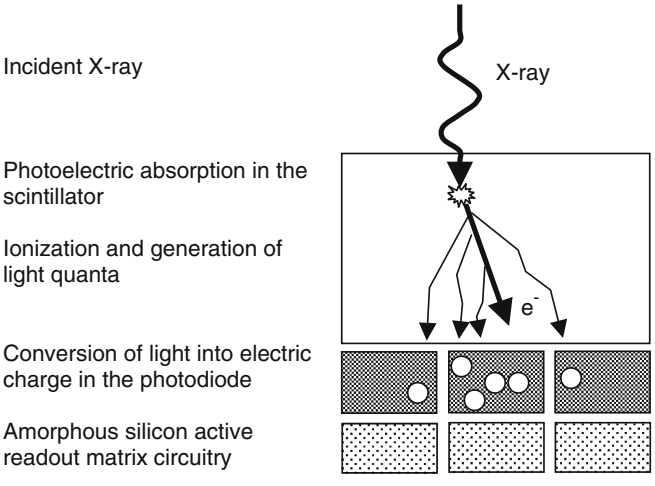

Fig. 2 Schematics of the indirect conversion process

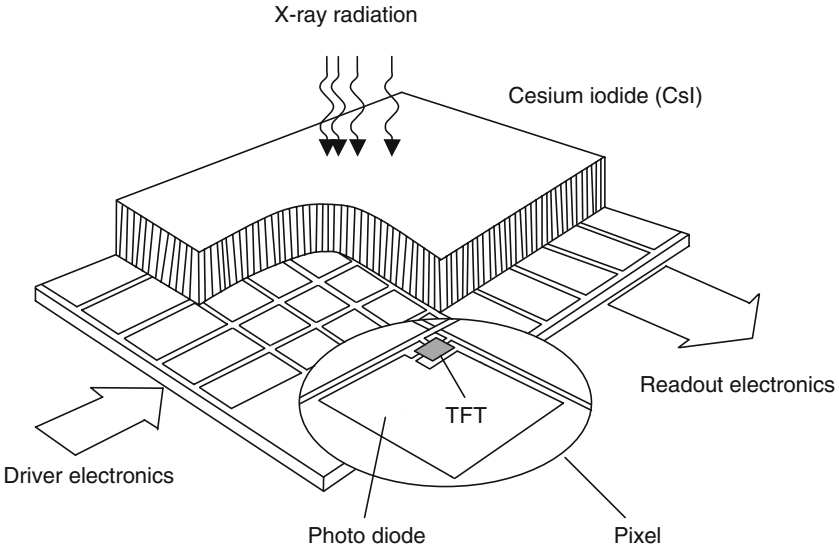

Fig. 3 Schematic view of an indirect converting flat detector based on CsI and an amorphous silicon active readout matrix

of electron-hole pairs which in turn recombine to produce photons in the visible range. Subsequently, this light hits the photodiode where it is converted to electric charge. This two-step conversion process has the advantage that both stages can be optimised relatively independently of one another. Figure 3 shows a schematic view of such a detector, described in detail in the following paragraphs.

The most commonly used scintillators are gadolinium oxysulfide (Gd_2O_2S) and thallium-doped cesium iodide (CsI:Tl)-CsI being the scintillator of choice. CsI can be grown as needle-shaped crystals measuring 5–10 μm in diameter. This needle–shaped structure acts as a light-guide and ensures that the light—emitted in the green part of the visible spectrum—reaches the photodiode with only little scatter. The other important feature of CsI is its very good X-ray absorption property (Fig. 4), related to the high atomic numbers of Z=55 and Z=53 for cesium and iodide, respectively. It is particularly suitable for applications in general radiography, angiography and fluoroscopy which require to cover a wide range of peak voltages from 45 kVp to 120 kVp. With an effective density of 3.6 g/cm^3, a CsI thickness of about 600 μm is typical for this range of applications. Even though CsI exhibits absorption minima near the K-edges around 35 keV (Fig. 4), CsI is also an adequate choice for flat detectors in mammography. Mammographic spectra, with typical peak voltages of between 25 and 30 kVp are dominated by the characteristic lines of the tube anode material (e.g. K_α at 17.5 keV and K_β at 19.6

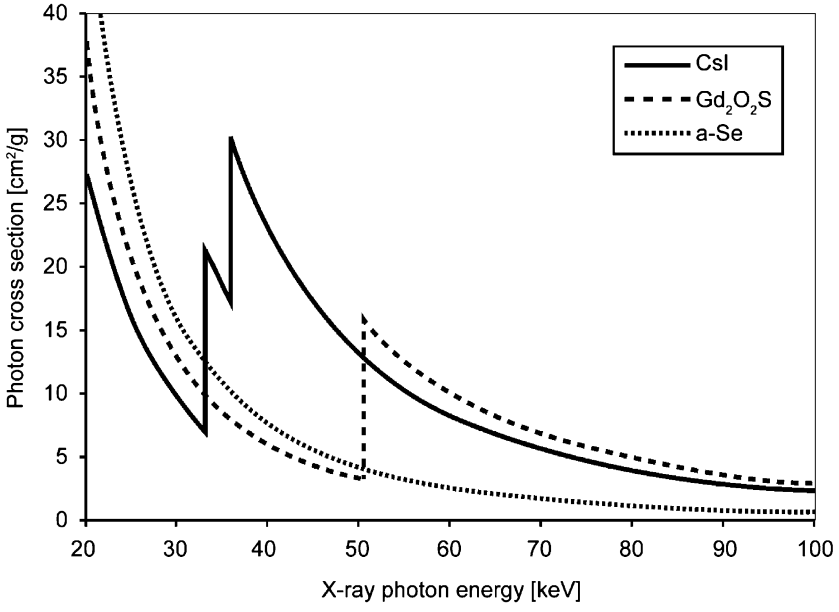

Fig. 4 Absorption coefficients of CsI, a-Se and Gd_2O_2S as a function of X-ray photon energy

keV for the commonly used molebdynum), well below the K-edges of CsI. A CsI thickness of about 150 μm is typical for that application and complies with the demand for good absorption and high resolution.

The photodiode is designed to reach a high quantum efficiency in the green part of the visible spectrum to match the spectrum of the scintillation light. Furthermore, it is optimised for high geometric aperture. At a pixel size of about 150 μm, the photodiode covers approximately 70% of the pixel area (geometric fill-factor) with current designs. Since the photons are subject to scatter processes in the CsI, however, the largest part of the signal is detected in the photodiode, no matter where the X-ray was absorbed in the continuous CsI layer in the first place. Therefore, one often refers to an effective fill-factor of 100% for all practical purposes. Taking all effects into account, an absorbed X-ray quantum with an energy of 60 keV generates a signal of approximately one thousand electrons.

The electric circuit for a TFT-based pixel structure is shown in Fig. 5. Its readout principle works as follows. First the photodiode, which acts as a capacitor, is charged to the full bias voltage prior to X-ray radiation with the TFT in its off-state. During X-ray radiation the converted optical photons are absorbed in the photodiode creating electron-hole pairs which drift to opposite contacts and gradually discharge the photodiode. The readout is initiated when the TFT is switched on via the gate line. It causes charge to flow to the photodiode so that its contact is restored to the data line voltage. The charge flow is measured in the external readout electronics and recorded as the signal. Since this step resets the photodiode to the full bias voltage the pixel is ready for the next acquisition.

The readout is performed row by row and addresses all pixels in the respective row simultaneously. Optimized low noise electronic circuits with high bandwidth are used to measure the charge and amplify the signal. These specifically designed chips may be connected to 120 or more individual readout channels. The readout chip also serves the function of a multiplexer which feeds the signals to an ADC (analog-to-digital converter). At this stage the signal is available for further processing in the image processing chain.

Flat detectors based on a direct conversion process

The direct detection process is depicted in Fig. 6. An X-ray which is absorbed in the photoconductor material generates a high energy electron. On its way through the material this electron creates many electron-hole pairs while losing its energy. An electric field is applied across the detection material to collect the generated charge carriers.

The following basic characteristics should be met by a material to qualify for a suitable direct converter: (1) high X-ray absorption, (2) large number of charge carrier generation per absorbed X-ray, (3) high collection efficiency of the charge carriers, and (4) low dark current. Photoconductor materials with a high atomic number and density and therefore good absorption characteristics, as, for example, lead iodide, lead oxide, cadmium telluride and mercury iodide are subject to current research [14–16]. The best understood and most frequently used material is, however, amorphous selenium (a-Se). It can be deposited directly onto an active matrix of amorphous silicon, where each pixel consists of an electrode and a TFT [3, 17].

Due to its low lying K-edge (Fig. 4), a-Se is particularly well suited for X-ray spectra used in mammography [18, 19]. An a-Se layer thickness of about 250 μm is sufficient for this application. For general radiography and even more so for fluoroscopy, however, adequate absorption can only be reached with an a-Se thickness of up to 1000 μm due to its relatively low atomic number (Z=34). One absorbed X-ray creates up to a thousand electron-hole pairs. By means of an applied electric field the electric charges are transported to the respective electrodes. On their way through

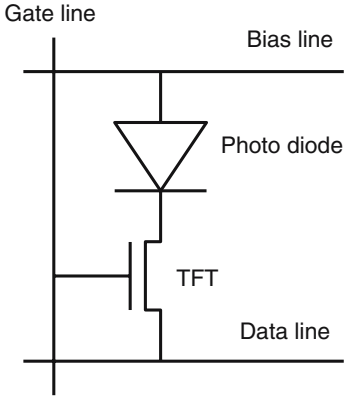

Fig. 5 Pixel circuit of an active matrix with photo diode and TFT switch for data readout

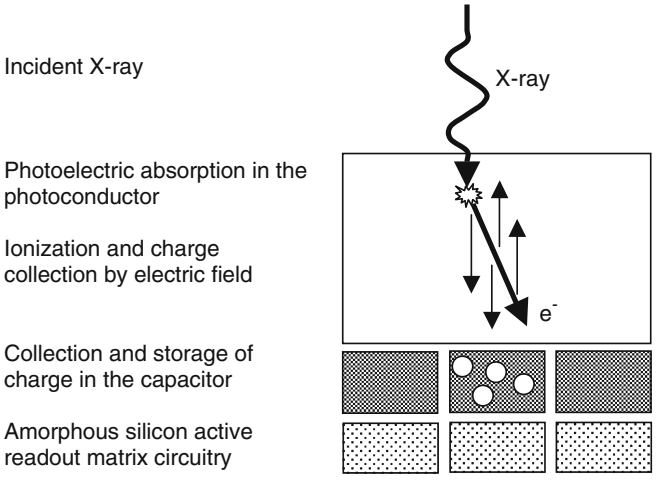

Fig. 6 Schematics of the direct conversion process

the material to the storage electrode of the pixel, part of the generated charge is lost by recombination or deep trapping. To obtain high charge collection efficiency, field strengths of about 10 V/μm are needed [18] which requires high voltages of approximately 10 kV applied across a 1000 μm thick a-Se layer. This in turn demands special care in the pixel design to protect the TFT from being damaged by high voltage discharge. A favorable ratio between drift length and diffusion length ensures that the charge which reaches the electrode is almost completely collected by the pixel located below the position where the X-ray quantum was initially absorbed.

The charge readout is accomplished by addressing the TFTs line by line, recharging the electrodes via the data line and measuring the respective signal in the peripheral low-noise readout electronics. The amplified signals are sequentially converted to digital signals via one or more ADCs. The signal is then fed to the image processing chain for further processing.

Performance characteristics of flat detectors

To characterize the performance of X-ray detectors in a transparent and reproducible way, a variety of physical measures have evolved. The most important performance parameters are (1) dynamic range, (2) MTF (modulation transfer function), (3) DQE, and (4) image lag. These high level parameters are fundamentally governed by a large set of lower level design and material parameters of the detector.

Figure 7 shows an example of a flat detector specifically developed for general radiography [10, 12]. This detector with an indirect conversion process is based on a CsI scintillator. With its active area of 43×43 cm^2 it is the largest of its kind and covers the most demanding sizes such as thorax and pelvis. The pixel size of 143×143 μm^2, optimised for high resolution required in radiography, leads to a square matrix of about 9 million pixels.

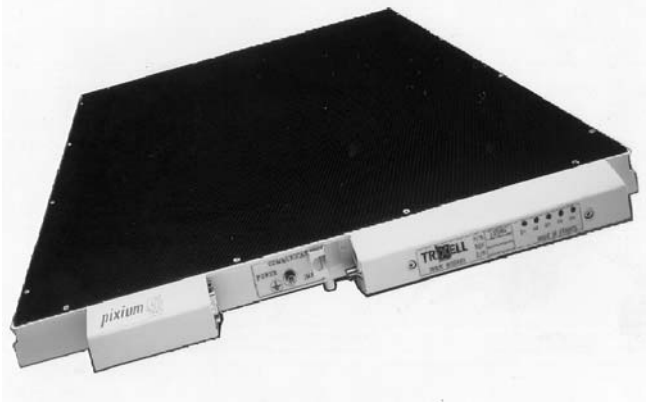

Fig. 7 Flat detector for radiographic applications with an active area of 43×43 cm^2 and a pixel size of 143×143 μm^2 (Pixium 4600, courtesy of Trixell, Moirans, France)

Dynamic range

Dynamic range is one of the key parameters characterizing the performance of X-ray detectors. The flat detector shown in Fig. 7—applying several 14 bit ADCs—exhibits very low electronic noise at a level of less than 1 digital unit. It shows a linear response as a function of dose (Fig. 8) and begins to saturate at a dose level of about 80 μGy. This allows a large dose range to be covered without the need for detector internal amplifier gain changes. Hence, the detector may not only be used at a standard dose level of 2.5 μGy (equivalent to 400 speed) but also at higher dose levels if highest image quality with respect to stochastic noise is required and at reduced dose levels (e.g. by 50%) which were demonstrated to be adequate for skeletal radiography [20]. Even much lower doses were shown to be useful for specific purposes such as the control of implants or search for foreign bodies [21]. Figure 8 also shows the response function for a screen-film system. Compared to the flat detector, its range of linear response is rather limited. This comparison demonstrates the advantage of flat detector technology over the conventional method since a much larger dose range can be addressed without risking wrong exposures. This feature reduces the need for retakes substantially which is particularly handy if external dose sensing devices are not available, for example in case of free exposures. A word of caution, however, is necessary, as the large dynamic range implies the risk to deliver higher dose to patients than necessary. Therefore it is mandatory to optimise the procedures in such a way that the right image quality is provided at the lowest possible dose.

In vascular imaging or cardiac angiography, an even broader dose range needs to be covered, ranging from very low system dose levels of about 10 nGy in fluoroscopy to much higher system dose levels of about 5 μGy in DSA (digital subtraction angiography). The need for this large dynamic range can be met by providing several detector internal modes, each one with a different amplification level at the input stage. The wide range of dose requirements is covered by selecting the detector mode which is appropriate for the expected signal range of the respective application.

Modulation transfer function

The MTF describes the detector's ability to transfer the input signal modulation of a given spatial frequency to its output. When defining the modulation of a digital (pixelized) detector one needs to take some care, as the measured modulation depends on the phase shift between the input signal and the pixel grid. Ambiguities are avoided by defining the pre-sampling MTF, i.e. the modulation before sampling but after convolution of the analog signal with the discrete sensor

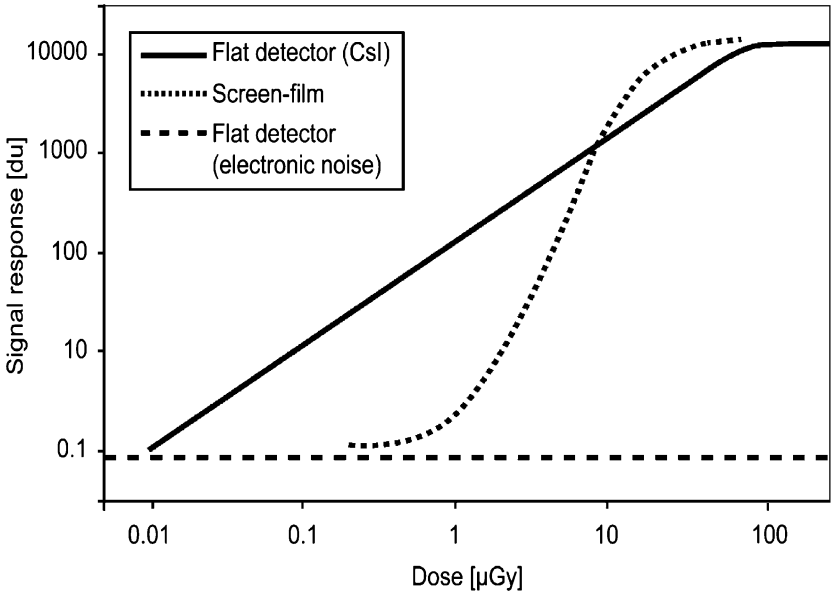

Fig. 8 Signal response of (1) a flat detector for radiographic applications with 14 bit analog-to-digital conversion and of (2) a screen–film system. For comparison, the electronic noise level of the flat detector is indicated as well

structure [22, 23]. The limiting function of a sensor of finite size is given by the Fourier transform of the pixel aperture a:

$$F(f) = \frac{\sin(\pi a f)}{\pi f} = a \cdot \sin c(af)$$

commonly referred to as the "sinc-function".

Figure 9 shows typical presampling MTFs for different technologies used in general radiography. The MTFs for screen-film systems and storage phosphor systems exhibit similar values over the spatial frequency range [24, 25]. Indirect converting flat detectors, based on CsI, show an improved MTF, particularly at higher spatial frequencies [12, 26]. Due to some degree of light scatter in the CsI the response function stays below the limiting sinc-function. This built-in low pass behavior has some advantages as described below. That feature applies to a much lesser extent to direct converting detectors based on a-Se where the applied electric field forces the generated charge to be almost completely collected in the one pixel below. Consequently, the MTF may come closer to the theoretical limit [27].

One important aspect of screen-film systems is that each sensitivity class (speed) matches a specific dose range. Increasing film speed, however, goes along with reduced resolution. This feature does not apply to flat detectors as their spatial resolution is—within their linear range—independent of the applied dose level.

Another important parameter of a digital imaging system is its limiting resolution. It is given by the Nyquist fre-

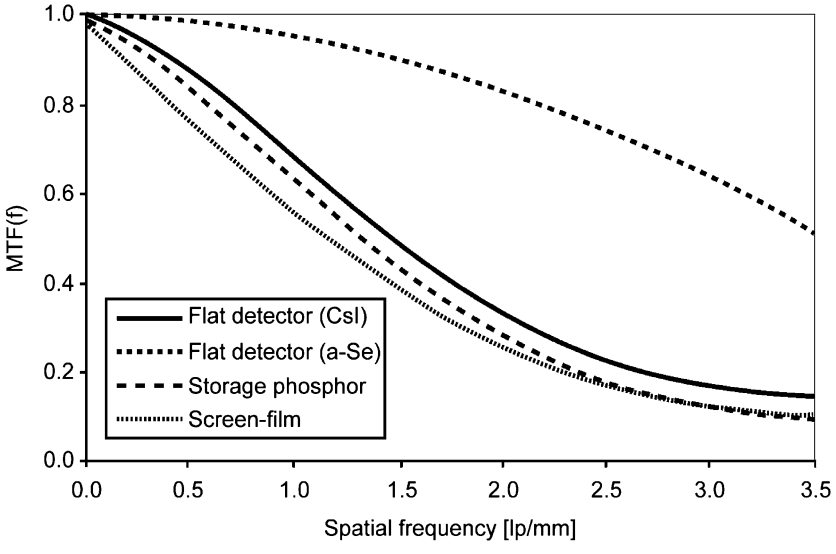

Fig. 9 Typical pre sampling MTF curves for different X-ray detectors used in general radiography applications: (1) flat detector with indirect conversion based on CsI, (2) flat detector with direct conversion based on a-Se, (3) storage phosphor with standard resolution and (4) screen–film system

quency, defined as $1/2d$ where d is the distance between two neighboring pixels. It represents the upper frequency limit at which spatial structures can be detected and above which aliasing effects occur. Aliasing not only effects the signal but also the noise. Hence, a MTF which does not reach the limit given by the sinc-function acts as a built-in low-pass filter. This is the case for the most frequently used scintillators such as CsI and Gd_2O_2S. The advantage is that aliasing and therefore back-folding of noise from the frequency region beyond the Nyquist frequency is partially suppressed—an important aspect to reach high DQE values at high spatial frequencies [28].

Detective quantum efficiency

DQE has become one of the fundamental physical parameters related to image quality [23, 29]. It refers to the efficiency of a detector to convert the X-ray radiation signal at its entrance window into a useful image signal. By definition, DQE compares the SNR (signal-to-noise ratio) at the detector output (digital signal) with that at the detector input (X-ray flux at the entrance window) as a function of spatial frequency f [8]:

$$\mathrm{DQE}(f) = \frac{\mathrm{SNR}^2(f)_{\mathrm{out}}}{\mathrm{SNR}^2(f)_{\mathrm{in}}} = \frac{q^2 G^2 \mathrm{MTF}^2(f)}{\mathrm{NPS}(f)}$$

DQE(f) is derived from the measured quantities MTF(f), noise power spectrum NPS(f), detector gain G, and the calculated average input quanta per unit area q. Since the SNR at the input corresponds to that of the ideal detector, DQE can reach a maximum value of 1.0. In practice, however, DQE is limited by the energy dependent quantum efficiency of the X-ray conversion layer.

Figure 10 shows DQEs for the most frequently used technologies in general radiography. Screen-film [24] and storage phosphor systems [25, 30] reach values between 20 and 30% at spatial frequencies below 1 lp/mm. Compared to screen-film, however, storage phosphor systems show a much more rapid fall-off at higher spatial frequencies. Higher DQE values are reached with direct converting flat detectors based on a-Se [27]. The highest DQE values, however, are obtained with indirect converting flat detectors based on CsI [12, 26]. Observer studies demonstrate that the high DQE values reached with the indirect converting flat detectors based on CsI correlate with (1) superior image quality (provided comparable system conditions are given) [31, 32], and (2) the potential to reduce dose without loss of image quality [33, 34], when compared to other technologies.

DQE is largely governed by the absorption properties of the converter material. Therefore it is worthwhile to briefly review the most commonly used X-ray converter materials for flat detectors in that respect. In what follows, quantum efficiencies are calculated for a CsI layer of 600 μm and an a-Se layer of 1000 μm (the thickest layers which have been reported for a-Se). Furthermore, a filtration of 4 mm Al and 0.2 mm Cu and a simulated object of 200 mm of poly (methyl methacrylate) are assumed. At 70 kVp quantum efficiencies of 77 and 67% are reached for CsI and a-Se, respectively. At higher peak voltages such as 120 kVp—typical for thoracic imaging—the relative advantage for CsI is even more pronounced. Here, quantum efficiencies of 52 and 37% are reached for CsI and a-Se, respectively.

In fluoroscopic imaging conditions very low signals have to be detected. The signal competes against the statistical noise as well as the additive electronic noise of the imaging

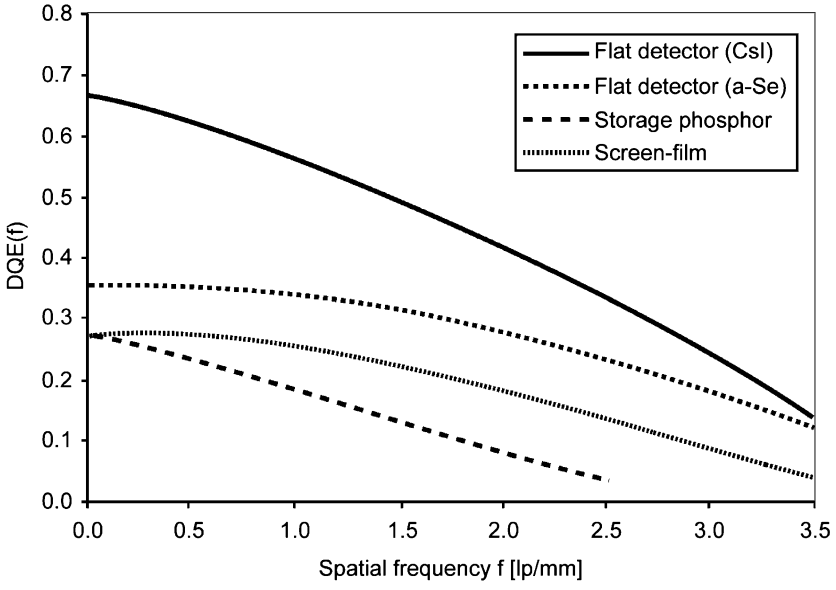

Fig. 10 DQE values of different X-ray detectors for general radiography: (1) flat detector with indirect conversion based on CsI, (2) flat detector with direct conversion based on a-Se, (3) storage phosphor with standard resolution and (4) screen–film system

chain. Hence, high absorption as well as high gain are essential under these circumstances. As these properties are in favor of CsI, this material qualifies particularly well for fluoroscopic imaging.

At the low end of the clinically relevant X-ray spectrum, a-Se has better absorption properties than CsI (see Fig. 4). This makes a-Se the ideal detector material for mammography, leading to the highest DQE. This statement is reflected by measurement results for two flat detectors, currently available with these two competing X-ray conversion materials. A detector based on a-Se/a-Si [35]—featuring a pixel size of 70 μm which corresponds to a Nyquist frequency of 7.2 lp/mm—exhibits significantly higher DQE values over the whole spatial frequency range than a detector based on CsI/a-Si [36] which has a pixel size of 100 μm, corresponding to a Nyquist frequency of 5 lp/mm.

Image lag

Image lag (sometimes called memory effect) may cause an increase in dark current and cause a reminiscent image after exposure [37]. This phenomenon results from the release of charge after the termination of the X-ray exposure: the charge which was trapped in metastable band-gap states in the a-Si active matrix or a-Se converter material during exposure is released afterwards slowly over time. Hence, lag is usually measured in subsequent non-exposed images as a function of elapsed time after an exposure or a series of exposures. The lag requirements on flat detectors built for real-time applications are high, as such detectors have to switch from high dose operations (e.g. DSA) to fluoroscopic dose levels within a very short time interval of about 1 s. As of today, the lowest values for lag are reached with the indirect converting flat detectors.

For a CsI/a-Si-based indirect converting flat detector designed for cardiac angiography—similar in technology as the one shown in Fig. 7—lag is measured to be about 0.3% after 1 s and below 0.04% after 10 s, using a detector mode with an integration time of 15 ms.

In comparison, lag values of about 6% after 1 s and around 1% after 10 s are reported for a direct converting flat detector based on a-Se/a-Si, applying similar integration times of 20 ms [38]. Such a high level of lag not only makes recursive offset subtraction methods necessary which may cut the effective frame rate of the system in half as every second frame is used for offset update. It also reduces the available dynamic range.

Advances in X-ray applications by flat detectors

Flat detectors play a central role in the evolution of diagnostic and interventional techniques in X-ray imaging. The advances fostered by flat detectors include improved image quality, new and better image processing techniques, true workflow-orientation and novel interventional techniques which use magnetic fields. The following sections provide an overview of the impact of flat detectors on workflow, progress in general radiography and mammography due to digital imaging processing, and new applications in real-time imaging (fluoroscopy and angiography).

Impact of flat detectors on workflow

A workflow-oriented environment requires several components which are well interwoven. Prerequisites are a RIS (radiology information system) and a PACS (picture archiving and communication system) environment, and an X-ray system that fully utilizes and supports both data infrastructures of the hospital. In this scenario, flat detector technology provides the missing link to support a fully digital environment.

Radiography which was—and to a large part still is—dominated by analog screen-film systems particularly profits from these developments. The following is a sketch of the steps that are necessary to establish a smooth workflow for a digital general purpose radiography system: A work list provided by the RIS is automatically loaded at the system's acquisition station. As soon as the correct patient name is selected from the work list, the corresponding examination is predefined and the system automatically starts the appropriate setup: the correct detector is selected (if the system includes more than one detector), tube and detector are moved to a predefined position in accordance to the first examination, the generator data and the tube collimators are preset, and the detector is prepared for acquisition. All of the necessary pre- and post-processing functions and parameters are also preselected. All of this takes place in the background while the patient is being positioned on the table or in front of the dedicated upright stand. As soon as the X-ray exposure has been taken the image is automatically processed and displayed immediately on the check monitor. In the meantime the system automatically selects the various predefined parameters for the next examination on the work list. Once all of the images have been acquired, they are automatically sent to the PACS and made available to all networked hospital departments or even to remote experts via teleradiology.

Workflow-oriented radiography systems based on flat detectors have been shown to reduce substantially the overall time required for nearly all examinations when compared to screen-film and storage phosphor based systems [39]. They thus play a central role in improving productivity in the radiology department.

Image processing techniques in general radiography and mammography

Image processing techniques provide the potential to improve image quality and to give way to new applications.

Three main areas can be distinguished: (1) optimised processing of single images to improve image quality, (2) synthesis of several images to enhance diagnostic content, and (3) automatic extraction of diagnostically important features.

The processing of single images takes a key position in digital radiography (Fig. 11) and mammography (Fig. 12). The diagnostic content of a digital image can be extracted in a way that is not accessible by analog film. Whereas flat detectors may cover a large dynamic range of, for example, 14 bits, the human eye cannot differentiate more than 7–8 bits of grey levels. Therefore an adequate reduction in the dynamics of the image signal is an important part of image processing. Also, techniques which enhance resolution or reduce noise are important features of image processing. Basic operations that meet these requirements include

- Dynamic range rescaling by an appropriate setting of the grey-scale window and level values. Segmentation techniques are used to remove unnecessary information by detecting the areas which are either subject to direct radiation or which are defined by the projected collimator. The resulting signal histogram, containing only the signal data of the object, is used to set appropriate window and level values or to extract other relevant information
- Grey scale mapping with non-linear characteristic functions to increase contrast in the region of interest while reducing it in other areas of lesser interest
- Dynamic range or density compression, defined in its simplest form by subtracting a given percentage of the low-pass filtered image (using very large filter kernels) from the original image. This technique allows one, for instance, to display the lung and the mediastinum of a thoracic image with high contrast. Similarly, this procedure lends itself to ideally display the chest wall and skin area of a mammogram simultaneously

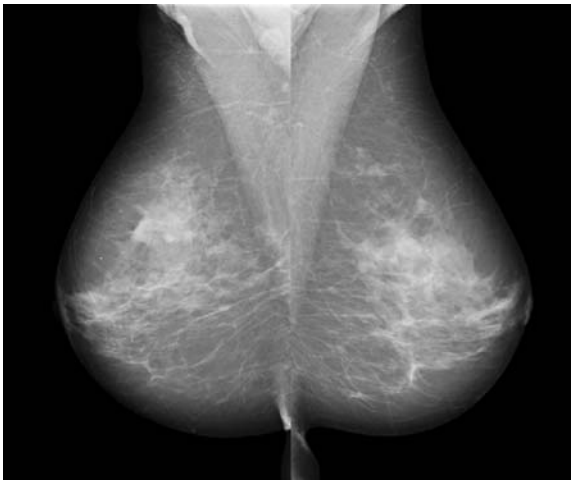

Fig. 12 Image examples of lateral mammograms acquired with a MAMMOMAT Novation (Siemens)

- Edge enhancement, a filtration method which improves the fine details of objects by applying a small kernel high-pass filter to the original image
- Multi-frequency filter techniques are a more general approach and may combine contrast enhancement, resolution improvements and noise reduction at the same time in the appropriate areas of the image. Here, the image is divided into several spatial frequency domains. Optimised filters are used in each frequency band, before the image is reconstructed. In addition, the filter parameters may be linked to the local image signal which may further improve the presentation of the diagnostic image content to the radiologist's eyes

Valuable additional information may be gained when synthesizing several images into one or several new images.

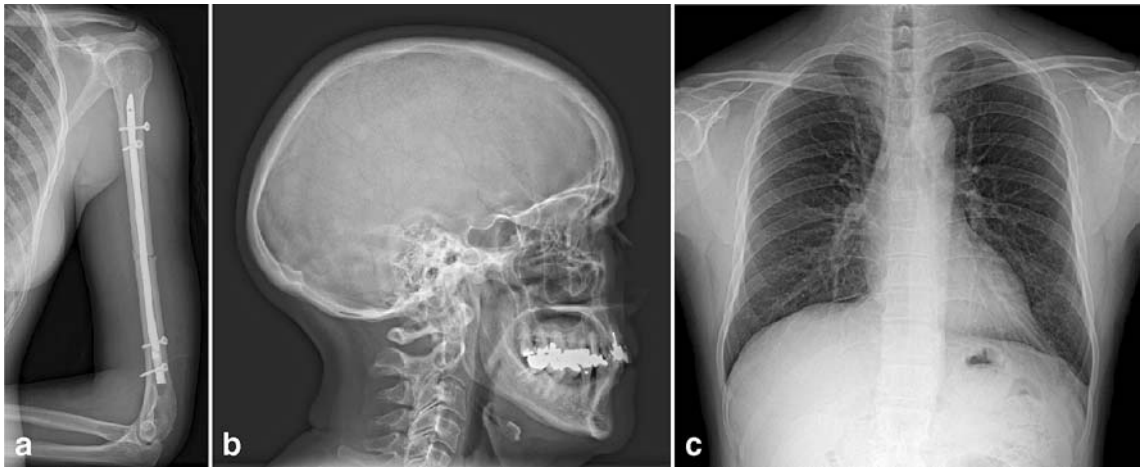

Fig. 11 Image examples of **a** an upper arm, **b** a skull and **c** a thorax a.p. acquired with an AXIOM Aristos MX system for general radiography (Siemens)

Image stitching is one such method which is used to create a new image larger than the detector area. Some of the applications, in particular full body scans of the upright standing patient, may require very fast consecutive image acquisitions because in most cases one is confronted with elderly and weaker patients. The flat detector's capability to support fast repetitive image acquisitions plays an essential role in such a procedure. To this end, several consecutive X-ray exposures are taken of the object so that a small overlap area between two neighboring images exists. The overlapping areas of the X-ray exposures are used by the image processing software to create seamless junctions. In this way, the complete spinal column or the entire skeleton can be displayed via a composed image. Special orthopedic image processing software allows to accurately measure and diagnose bone defects.

Another technique is the dual energy method which takes advantage of the energy dependence of the mass absorption coefficient. Here, two X-ray images are gathered, using very different X-ray spectra. By adequate linear superposition of the images, different types of tissue may be displayed selectively. Again, flat detectors are ideally suited for this application as they allow acquisition of the two images within a very short time interval which helps to keep motion artefacts at a low level. In thoracic diagnostics, for example, the soft tissue (lung parenchyma, mediastinum) or the structures containing calcium (bone, calcifications) may be displayed separately. This method may prove advantageous for displaying tumors. Whether or not it will have a future is open-ended, since computed tomography represents a superior and well-established alternative for this kind of application.

Quasi 3D information can be achieved by digital tomosynthesis [40]. With this technique one acquires a series of projection images (typically 10–30) in a given angular range (e.g. −20 to +20°). In a post-processing step these images are used to reconstruct the 3D data set, applying similar algorithms as the ones used in computed tomography. Here, though, the spatial resolution in the direction normal to the detector is much lower than in the directions parallel to the detector plane. Presently, the main focus of applications is on mammography with the goal to visualize the 3D spatial distribution of calcifications and to improve the detectability of masses. Other applications in general radiography may include the diagnosis of arthritis in finger joints or lung nodules.

In the future, CAD (computer aided detection) methods will play a more and more important role of feature extraction from individual images. One such application is the detection of tumors in thoracic images. To date, however, it is difficult to say how long it will take until established methods are available, especially in view of the complexity involved in detecting tumors in thoracic radiographs [41]. For digital mammography, the breakthrough of CAD methods is closer to reality and may even accelerate its acceptance. CAD systems, known to supply consistent quality (parameters—humans are influenced by—such as the time of day or the work load, do not exist for such systems) have continuously shown improved sensitivity and specificity over the past years. Although this topic is still discussed controversially [42], there is no doubt that in taking the role of a "second opinion", the technology very efficiently supports radiologists in their diagnosis.

New applications in angiography and fluoroscopy

Real-time X-ray imaging systems are used for a wide spectrum of clinical applications. Such systems range from mobile X-ray systems for surgery and over- and undertable fluoroscopy systems (e.g. for examinations of the gastrointestinal tract) to angiography systems equipped for the diagnosis of vessel pathologies and minimally invasive treatment. Moreover, the field of angiography includes special systems for cardiology and neurology.

The image intensifier which has been the technology of choice for these systems has matured over the past decades allowing for high-quality X-ray examinations and interventions. The X-ray dose required for examinations or interventions was successively reduced, decreasing at the same time the X-ray exposure to both patient and user. Therefore, all new detector technologies are measured against the level of quality standard established by image intensifiers.

However, image intensifier technology also has a number of disadvantages. The mapping of the convex input screen onto the planar output fluorescent screen leads to image distortions especially along the rim of the image and consequently to non-homogeneous image quality across the image. Scatter processes of light and electrons within the image intensifier limit the coarse contrast resolution (veiling glare). Yet another critical point with large image intensifier formats is patient access as well as the flexibility during angulation of the image intensifier at the C-arm due to the large size and depth of the vacuum tube. Also, the amplification principle of image intensifiers based on internal electric fields prohibits their usage in the vicinity of strong magnetic fields. Finally, large-format image intensifiers did not succeed in replacing screen-film bucky trays in fluoroscopy systems to cover radiography applications. The reasons for this being the round image format, the large depth of the image intensifier tube, and a limited DQE at the high exposure levels required for radiographic exposures.

Flat detectors for real-time imaging [11, 43–47] either avoid or at least reduce some of the disadvantages of image intensifiers. The most important technical advantages of flat detectors are summarized below:

- Homogeneous image quality across the entire image area resulting in distortion-free images and position-independent spatial resolution
- High "low contrast resolution"

- High DQE across all dose levels, particularly for CsI/aSi-based flat detectors
- High dynamic range, covering all dose levels from fluoroscopy to DSA
- Square or rectangular active areas which, together with the flat and compact design, improve the accessibility of the patient
- Compatibility with environments where strong magnetic fields are required

These advantages suggest that X-ray systems with flat detectors have the potential to improve further the existing applications and give way to new diagnostic and interventional techniques. The following three examples shall underline this statement.

The improved detectability of small structures such as the tip of the catheter due to increased contrast resolution may lead to shorter examination times. This in turn should reduce the integrated applied dose. In cardiac angiography the improved visibility of stents allows, for example, to use hand injections of contrast medium for left ventriculograms, which reduces the contrast medium load for the patient.

3D views of body regions generate additional information for diagnosis and facilitate orientation during interventions. Today 3D visualization is a standard feature for interventions in neuroradiology. The treatment of aneurysms and arteriovenous malformations through coils or other embolization methods has been in use for years, using image intensifier based X-ray systems. These methods, however, will largely benefit from flat detectors due to the rectangular image format, the high spatial resolution and the distortion-free images. The high dynamic range and the good contrast resolution will enable to enhance the soft tissue resolution and may allow to probe into some of the classic applications of computed tomography.

The flat detectors' compatibility with strong magnetic fields supports magnetic catheter navigation which is a

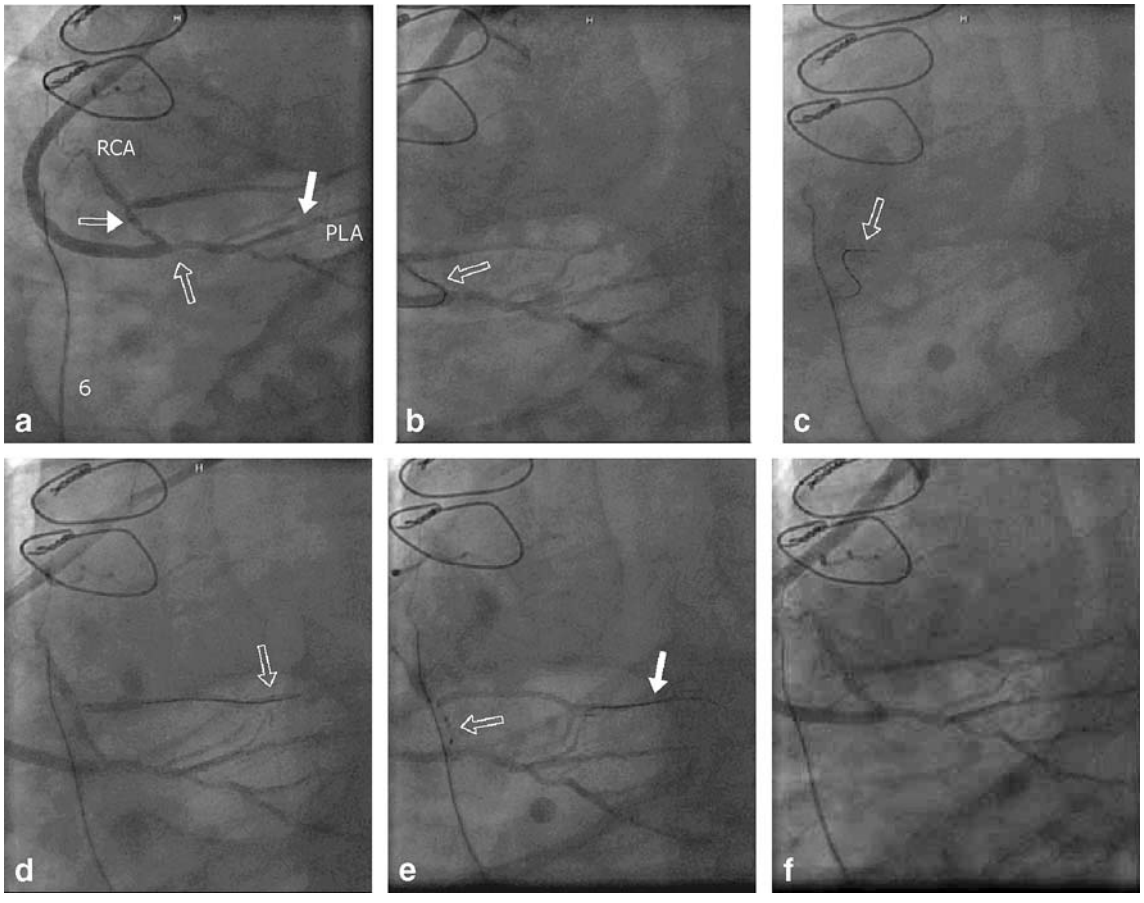

Fig. 13 Highly symptomatic patient with three stenoses beyond a previous vein graft in the right coronary artery (RCA) and associated vessels. Angiograms acquired with an AXIOM Artis *d*FC Magnetic Navigation (Siemens). **a** Angiography with all three lesions identified: (1) at graft anastomosis, (2) in the posterior lateral artery (PLA) and (3) in the RCA very close to the bifurcation. **b** Wire turning retrograde into RCA out of veingraft. **c** Wire bending from RCA into acute marginal branch without removing wire for reshaping. **d** Wire anchored in acute marginal branch. **e** Balloon at third lesion in the RCA very close to the bifurcation. Wire anchored into distal acute marginal branch. **f** Post-PTCA of all three lesions

unique new technology platform for electrophysiology and interventional cardiology [48]. With the help of two magnets, providing a magnetic field of up to 0.1 Tesla, the clinician can accurately navigate catheters and guidewires through the vessels and the chambers of the heart. Rotating the magnets independently changes the local magnetic field at the position of the catheter whose tip is equipped with a tiny magnet. As a result, the catheter changes orientation into the desired direction within the vascular tree. The guiding is supported by the flat detector which is used to acquire two perpendicular X-ray projection images showing the catheter and the vessel structure. By drawing the new intended direction of the catheter directly onto the projection images, the new required local magnetic field can be calculated and set up by moving the magnets into their new positions. This allows to perform difficult navigation tasks such as moving along a calcified vessel which can now be performed with softer catheters minimizing the traumatization of the vessel, changing direction at a bifurcation (in particular if the branch point itself is stenosed), or other hard-to-navigate sections in the vascular or cardiac system.

This method may revolutionize the work of cardiologists and radiologists in the near future. Several applications are in the focus of interest. One problem which can be addressed with the new technology is the chronic blockage of the cardiac vasculature, which so far has always fallen into the domain of cardiac surgery. With the new system, opening the chronic total occlusion may be addressed without surgery. Figure 13 shows a case of a highly symptomatic patient with three stenoses beyond a previous vein graft in the right coronary artery and associated vessels. That patient was treated by magnetically guided PTCA (percutaneous transluminal coronary angiography) of the three stenoses in the right coronary artery. Another disease to be addressed is complex arrhythmia, such as fibrillation in the left atrium. Here, the system is used to apply radiofrequency ablation of the arrhythmogenic tissue in the atrium. A further area of focus is in the field of serious cardiac insufficiencies where pacemakers are used to stimulate both chambers of the heart. With this new technology, present problems to navigate the probe electrodes into the optimum positions through the veins may be overcome. An even other field may be applications where medical devices such as drug-eluting stents need to be placed at small and tortuous side-branches, requiring support by magnetic assisted navigation.

Future developments

The exciting technology of flat detectors is subject to continuous further development and improvement. Miniaturized electronics allow for even flatter and lighter detectors required for mobile or portable applications. External cooling, still needed in some real-time applications today, will be overcome in the future.

Another area of progress relates to the improvement of the signal-to-noise ratio. This can be obtained through vertical pixel structures. In case of indirectly converting flat detectors the photodiode and switching transistors are stacked on top of each other instead of being located next to each other as in present and past designs. With such a "maximum fill-factor" approach, the active area of the photodiode is enlarged, allowing to detect nearly all of the generated optical photons and therefore maximizing the signal. The objective of developing new direct conversion materials such as lead iodide, cadmium telluride or mercuric iodide is to improve the absorption characteristics and the overall signal in order to enhance signal-to-noise, resolution and in consequence DQE. Higher bit depths of 16 or 18 bits could improve 3D applications, allowing to probe further into the domain of computed tomography which is the prime standard for low contrast X-ray imaging today.

In the future, pixel arrays based on CMOS (complementary metal oxide semiconductor) technology may be the basis for further progress. Several steps can be envisioned. In the integrating domain, pixel structures including a photodiode and a switch transistor (indirect conversion) or an electrode plus switch transistor (direct conversion) are straight forward designs. Including an amplification stage for each pixel is an improvement which helps to increase the signal-to-noise ratio. One step further could involve counting structures, where each absorbed X-ray quantum is detected individually and registered accordingly. Methods of this kind would allow to generate a quasi noise-free signal processing chain; only quantum statistics would remain as the sole contributor of noise. Photon counting has already been demonstrated for mammography [49], even though this approach does not involve a full field detector but a linear detector in a scanning mode. If in addition to counting the quanta, the X-ray's energy were detected as well, it would be possible to imagine new applications based on energy discriminating methods ("color imaging").

Each new development, be it technical or application-oriented, will be ultimately judged on the basis of its benefit for the patient or the treating physician. Some of the key factors determining the criteria will be workflow, image quality and a careful usage of dose.

Acknowledgements The author would like to thank Prof. G. Marchal (University Hospitals Leuven, Belgium) for providing the radiographic images. The mammograms are courtesy of Dr. R. Schulz-Wendtland (University of Erlangen, Germany). Dr. R. Meese (Mother Frances Hospital, Tyler, Texas, USA) provided the case using magnetic navigation techniques. Also special thanks goes to Dr. P. Bernhardt who provided the simulated data on quantum efficiencies and to Dr. T. Mertelmeier for his suggestions and availability for fruitful discussions.

References

1. Antonuk LE (1993) Thin-film, flat imagers—a coming revolution in megavoltage and diagnostic imaging? Phys Med 9:63–68
2. Chabbal J, Chaussat C, Ducourant T, Fritsch L, Michailos J, Spinnler V, Vieux G, Arques M, Hahm G, Hoheisel M, Horbaschek H, Schulz R, Spahn M (1996) Amorphous silicon X-ray image sensor. Proc SPIE 2708:499–510
3. Lee DL, Cheung LK, Jeromin LS (1995) A new detector for projection radiography. Proc SPIE 2432:237–249
4. Street RA (2000) Technology and applications of amorphous Silicon. Springer Series in Material Science. Springer, Berlin Heidelberg New York, pp 47–221
5. Weisfield RL, Hartney M, Schneider R, Alfatooni K, Lujan R (1999) High performance amorphous silicon image sensor for X-ray diagnostic medical imaging applications. Proc SPIE 3659:307–317
6. Zhao W, Rowlands JA (1995) X-ray imaging using amorphous selenium: feasibility of a flat self-scanned detector for digital radiology. Med Phys 22:1595–1604
7. Noel A, Thibault F (2004) Digital detectors for mammography: the technical challenges. Eur Radiol 14:1990–1998
8. Beutel J, Kundel HL, Van Metter RL (2000) Handbook of medical imaging. Vol. 1: Physics and Psychophysics. SPIE Press
9. Antonuk LE, El-Mohri Y, Siewerdsen JH, Yorkston J, Huang W, Scarpine VE, Street RA (1997) Empirical investigation of the signal performance of a high-resolution, indirect detection, active matrix flat imager (AMFPI) for fluoroscopic and radiographic operation. Med Phys 24:51–70
10. Chaussat C, Chabbal J, Ducourant T, Spinnler V, Vieux G, Neyret R (1998) New CsI/a-Si 17″×17″ X-ray flat detector provides superior detectivity and immediate direct digital output for General Radiography systems. Proc SPIE 3336:45–56
11. Granfors PR, Albagli D, Tkaczyk JE, Aufrichtig R, Netel H, Brunst G, Boudry J, Luo D (2001) Performance of a flat cardiac detector. Proc SPIE 4320:77–86
12. Spahn M, Strotzer M, Völk M, Böhm S, Geiger B, Hahm G, Feuerbach S (2000) Digital radiography with a large-area, amorphous-silicon, flat X-ray detector system. Invest Radiol 35:260–266
13. Yamazaki T, Tamura T, Nokita M, Okada S, Hayashida S, Ogawa Y (2004) Perforamance of a novel 43-cm×43-cm flat-panel detector with CsI:Tl scintillator. Proc SPIE 5368:379–385
14. Mainprize JG, Hunt DC, Yaffe MJ (2002) Direct conversion detectors: the effect of incomplete charge collection on detective quantum efficiency. Med Phys 29:976–990
15. Simon M, Ford RA, Franklin AR, Grabowski SP, Menser B, Much G, Nascetti M, Overdick M, Wiechert DU (2004) PbO as direct conversion X-ray detector material. Proc SPIE 3659:188–199
16. Street RA, Ready SE, Melekhov L, Ho J, Zuck A, Breen B (2002) Approaching the theoretical X-ray sensitivity with HgI2 direct detection image sensors. Proc SPIE 4682: 414–422
17. Polischuk B, Rougeot H, Kerwin W, Debrie A, Poloquin E, Hansroul M, Martin JP, Truong TT, Choquette M, Laperrière L, Shukri Z (1999) Direct conversion detector for digital mammography. Proc SPIE 3859:417–425
18. Kasap SO, Rowlands JA (2002) Direct-conversion flat X-ray image sensors for digital radiography. IEEE 90:591–604
19. Stone MF, Zhao W, Jacak BV, O'Connor P, Yu B, Rehak P (2002) The X-ray sensitivity of amorphous selenium for mammography. Med Phys 29:319–324
20. Völk M, Strotzer M, Holzknecht N, Manke C, Lenhart M, Gmeinwieser J, Link J, Reiser M, Feuerbach S (2000) Digital radiography of the skeleton using a large-area detector based on amorphous silicon technology: image quality and potential for dose reduction in comparison with screen-film radiography. Clin Radiol 55:615–621
21. Völk M, Strotzer M, Gmeinwieser J, Alexander J, Fründ R, Seitz J, Manke C, Spahn M, Feuerbach S (1997) Flat X-ray detector using amorphous silicon technology: reduced radiation dose for the detection of foreign bodies. Invest Radiol 32:373–377
22. Dobbins JT III (1995) Effects of undersampling on the proper interpretation of modulation transfer function, noise power spectra, and noise equivalent quanta of digital imaging systems. Med Phys 22:171–181
23. Stierstorfer K, Spahn M (1999) Self-normalizing method to measure the detective quantum efficiency of a wide range of X-ray detectors. Med Phys 26:1312–1319
24. Van Metter R, Dickerson R (1994) Objective performance characteristics of a new asymmetric screen-film system. Med Phys 21:1483–1490
25. Dobbins JT III, Ergun DL, Rutz L, Hinshaw DA, Blume H, Clark DC (1995) DQE(*f*) of four generations of computed radiography acquisition devices. Med Phys 22:1581–1593
26. Granfors PR, Aufrichtig R (2000) DQE(*f*) of an amorphous Silicon flat X-ray detector: detector parameter influences and measurement methodology (2000) Proc SPIE 3977:2–13
27. Lee DL, Cheung LK, Rodricks B, Powell GF (1998) Improved imaging performance of a 14×17-inch Direct Radiography system using Se/TFT detector. Proc SPIE 3336:14–23
28. Moy JP (1998) Image quality of scintillator based X-ray electronic imagers. Proc SPIE 3336:187–194
29. Metz CE, Wagner RF, Doi K, Brown DG, Nishikawa RM, Myers KJ (1995) Towards consensus on quantitative assessment of medical imaging systems. Med Phys 22:1057–1061
30. Nakano Y, Gido T, Honda S, Maezawa A, Wakamatsu H, Yanagita T (2002) Improved computed radiography image quality from a BaFl:Eu photostimulable phosphor plate. Med Phys 29:592–597
31. Hamers S, Freyschmidt J, Neitzel U (2001) Digital radiography with a large-scale electronic flat-panel detector vs screen-film radiography: observer preference in clinical skeletal diagnostics. Eur Radiol 11:1753–1759
32. Kotter E, Langer M (2002) Digital radiography with large-area flat-panel detectors. Eur Radiol 12:2562–2570
33. Völk M, Hamer OW, Feuerbach S, Strotzer M (2004) Dose reduction in skeletal and chest radiography using a large-area flat-panel detector based on amorphous silicon and thallium-doped cesium iodide: technical background, basic image quality parameters, and review of the literature. Eur Radiol 14:827–834
34. Ludwig K, Henschel A, Bernhardt TM, Lenzen H, Wormanns D, Diederich S, Heindel W (2003) Performance of a flat-panel detector in the detection of artificial erosive changes: comparison with conventional screen-film and storage-phosphor radiography. Eur Radiol 13:1316–1323
35. Yorker JG, Jeromin LS, Lee DLY, Palecki EF, Golden KP, Jing Z (2002) Characterization of a full field mammography detector based on direct X-ray conversion in selenium. Proc SPIE 4682:21–29

36. Vedantham S, Karellas A, Suryanarayanan S et al. (2000) Full breast digital mammography with an amorphous silicon-based flat panel detector: physical characterization of a clinical prototype. Med Phys 27:558–567
37. Yorkston J (2004) Specifications, performance evaluation, and quality assurance of radiographic and fluoroscopic systems in the digital era. AAPM Summer School Proceedings. Medical Physics Monograph No. 30:177–228
38. Loustauneau V, Bissonnette M, Cadieux S, Hansroul M, Masson E, Savard S, Polischuk B (2004) Ghosting comparison for large-area selenium detectors suitable for mammography and general radiography. Proc SPIE 5368:162–169
39. DeMaster DR (2001) Digital radiography offers major productivity gains over computed radiography: results of time–motion study. Appl Radiol 30:28–31
40. Dobbins JT III, Godfrey DJ (2003) Digital X-ray tomosynthesis: current state of the art and clinical potential. Phys Med Biol 48:R65–R106
41. Van Ginneken B, ter Haar Romeny BM, Viergever MA (2001) Computer-aided diagnosis in chest radiography: a survey. IEEE 20:1228–1241
42. Hendee WR (1999) In the next decade automated computer analysis will be an accepted sole method to separate "normal" from "abnormal" radiological images. Med Phys 26:1–4
43. Bruijns T, Bastiaens R, Hoornart B, von Reth E, Busse F, Heer V, Ducourant T, Cowen A, Davies A, Terrier F (2002) Image quality of a large area dynamic flat detector: comparison with a state of the art II/TV system. Proc SPIE 4682:332–343
44. Busse F, Rütten W, Sandkamp B, Alving PL, Bastiaens R, Ducourant T (2002) Design and performance of a high-quality cardiac flat detector. Proc SPIE 4682:819–827
45. Choquette M, Demers Y, Shukri Z, Tousignant O, Aoki K, Honda M, Takahashi A, Tsukamoto A (2001) Real time performance of a selenium-based detector for fluoroscopy. Proc SPIE 4320:501–508
46. Colbeth RE, Boyce S, Fong R, Gray K, Harris R, Job ID, Mollov I, Nepo B, Pavkovich J, Taie-Nobarie N, Seppi EJ, Shapiro EG, Wright MD, Webb C, Yu JM (2001) 40×30 cm^2 flat imager for angiography, R&F and cone-beam CT applications. Proc SPIE 4320:94–102
47. Suzuki K, Ikeda S, Ishikawa K, Iinuma G, Ogasawara S, Moriyama N, Konno Y (2002) Development and evaluation of a digital radiography system using a large-area flat detector. Proc SPIE 4682:363–370
48. Faddis MN, Blume W, Finney J, Hall A, Rauch J, Sell J, Bae KT, Talcott M, Lindsay B (2002) Novel, magnetically guided catheter for endocardial mapping and radiofrequency catheter ablation. Circulation 106:2980–2985
49. Lundqvist M, Danielsson M, Cederström B, Chmill V, Chuntonov A, Aslund M (2003) Measurements on a full-field digital mammography system with a photon counting crystalline silicon detector. Proc SPIE 5030:547–552